

# A global line list for HDO between 0 and 35000 cm<sup>-1</sup> constructed using multiphoton spectra

Nikolay F. Zobov<sup>a</sup>, Maksim A. Koshelev<sup>a</sup>, Dmitry S. Makarov<sup>a</sup>, Vladimir Yu. Makhnev<sup>a</sup>, Oleg V. Boyarkin<sup>b</sup>, Vladimir G. Tyuterev<sup>c</sup>, Jonathan Tennyson<sup>d</sup>, Oleg L. Polyansky<sup>\*,d,a</sup>

<sup>a</sup>*Institute of Applied Physics, Russian Academy of Sciences, Ulyanov Street 46, Nizhny Novgorod 603950, Russia*

<sup>b</sup>*École Polytechnique de Lausanne, Switzerland*

<sup>c</sup>*Groupe de Spectrométrie Moléculaire, University of Reims, France*

<sup>d</sup>*Department of Physics and Astronomy, University College London, London, WC1E 6BT, UK*

---

## Abstract

Multiphoton spectroscopy of monodeuterated water is employed to determine more than 210 new energy levels of HDO in the 25 000 – 35 000 cm<sup>-1</sup> region. These new empirical energy levels are used to fit a potential energy surface (PES) valid between 20 000 cm<sup>-1</sup> and 35 000 cm<sup>-1</sup>. Using this PES and an accurate lower energy PES as starting points, an energy-switching surface is constructed which is capable of reproducing the whole HDO spectrum from 0 to 35 000 cm<sup>-1</sup>. This PES is used to calculate a line list for HDO which covers infra red, visible and near ultraviolet transitions.

---

---

\*Corresponding author

*Email address:* o.polyansky@ucl.ac.uk (Oleg L. Polyansky)

## 1. Introduction

Even though  $\text{H}_2$  and  $\text{CO}$  are more abundant in the Universe than water,  $\text{H}_2^{16}\text{O}$  is one of the most important molecule both on Earth and in the Universe as a whole. Deuterated water makes a small, but not insignificant, contribution to the absorption of light by water in the Earth's atmosphere. In particular, deuteration leads to large shifts in transition frequencies and therefore absorption by deuterated water often occurs in what are known as the water transparency windows due to the absence of absorption by  $\text{H}_2^{16}\text{O}$ . In addition, HDO spectra has long been used on both the Earth [1–9] and other planets [10, 11] as a means to understand their climatic evolution. The increased relative abundance of deuterium on Venus leads to particularly strong HDO spectra [12]. HDO is also well known in cometary spectra [13, 14].

Unlike  $\text{H}_2^{16}\text{O}$  [15, 16] and  $\text{H}_2^{17,18}\text{O}$  [17], there are no global deuterated water HDO line lists. The most extensive published  $\text{HD}^{16}\text{O}$  line list, the VTT line list due to Voronin *et al.* [18], only gives systematic coverage up to  $25\,000\text{ cm}^{-1}$ .

Previously, we have analyzed the  $\text{H}_2^{16}\text{O}$  spectrum up to dissociation [19–25] and used these data to produce a global potential energy surface (PES) for  $\text{H}_2^{16}\text{O}$  [16]. The global  $\text{H}_2^{16}\text{O}$  PES was used to compute a widely-used, global line list which considers rotational states with  $J \leq 72$  and includes all the rovibrational states of water up to dissociation [16]. This global line list is thus applicable for any temperature for which the noticeable amount of water monomer is present as well as non local thermodynamic equilibrium (non-LTE) applications.

The situation for HDO study is much less developed. Until the present study, experimentally-determined HDO energy levels only extend up to 23 000  $\text{cm}^{-1}$  [26, 27]; see the IUPAC database [28] for a comprehensive survey experimental HDO spectra and compilation of energy levels. Rotationally excited levels up to  $J=30$  were determined empirically from hot HDO emission spectra [29, 30]. Besides these conventional spectroscopic studies, HDO transition frequencies were also measured using action spectroscopy and a laser double resonance technique [31]. These data were not included into IUPAC database but were used in the construction of the best currently available semi-empirical PES [32] for HDO; this PES is limited to energies below 25 000  $\text{cm}^{-1}$ . Experimentally determined energy levels of water isotopologues above this level and up to dissociation are important not only for characterising the global PES but also for quantifying non-Born-Oppenheimer effects in the near dissociation region; these effects remain to be determined by either theory or experiment for any polyatomic system.

For modelling atmospheric absorption, astrophysics and other applications knowledge of energy levels alone is not sufficient. These studies require both line centers and line intensities; these constitute a line list which can be computed using a PES and dipole moment surface (DMS) [33]. A very accurate water DMS called, LTP2011 [34], was used to compute line intensities with sub-percent accuracy for many bands of  $\text{H}_2^{16}\text{O}$  [16, 35, 36], as well as all deuterated isotopologues of water, namely  $\text{HD}^{16,17,18}\text{O}$ , and  $\text{D}_2^{16,17,18}\text{O}$  [37]. The DMS for water has been improved by more extensive *ab initio* calculations giving the CKAPTEN DMS [38]. CKAPTEN allows  $\text{H}_2^{16}\text{O}$  line intensities to be reproduced in the infrared (IR), optical and, in particular,

the near ultra-violet (UV) regions with better accuracy [39, 40]. Both these DMSs are employed below. We note that there are no measurements of HDO line intensities with sub-percent accuracy. We assume that, as for  $\text{H}_2^{16}\text{O}$ , the HDO line intensities will be more accurate with the CKAPTEN DMS.

Although a comprehensive HDO linelist is necessary for a number of applications, it is not needed for energies up to dissociation.  $35\,000\text{ cm}^{-1}$  represents the highest wavenumber for which a single photon spectrum of  $\text{H}_2\text{O}$  has been observed [41]; it thus provides a logical upper limit for an HDO line list. Here we report the measurements that employ a triple resonance vibrational overtone excitation to probe rovibrational levels up to  $35\,000\text{ cm}^{-1}$  in HDO. We fit these data to obtain a fitted PES that is valid for these energies. We use this PES to calculate a line list, which considers states up to  $35\,000\text{ cm}^{-1}$ .

The paper is organized as follows. We describe our experiment in Section 2. Section 3 provides analysis and assignment of the experimental data. Section 4 describes the procedures that were used for fitting, an energy switching function and presents our global HDO PES. Section 5 gives the line list calculations that use the newly constructed PES. We give our conclusions in section 6.

## 2. Experimental method

We employ a triple resonance vibrational overtone excitation scheme to access molecular states of gas-phase HDO with total energy above the lowest dissociation threshold and laser-induced fluorescence to detect the appearing OH fragments. The details of the experimental apparatus and method can be found elsewhere [19, 20, 42]. Four tunable dye lasers of 6–10 ns duration

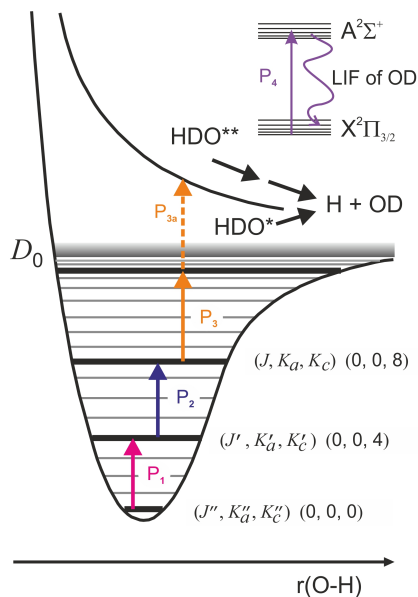


Figure 1: Schematic energy diagram for the state-selective triple resonance vibrational overtone excitation of HDO to the high-lying energy levels below the lowest dissociation threshold  $D_0$  with subsequent detection of OD fragments via LIF.

are employed in this method (Figure 1). A photon from the first laser ( $P_1$ ) promotes a fraction of the water vapor molecules in a chosen rotational state of the ground vibrational level to a level that contains 4 vibrational quanta in the OH stretch. About 10 ns later a photon of the second laser ( $P_2$ ) promotes up to half of these pre-excited molecules to a second intermediate level that corresponds to 8 quanta of OH-stretch, the gateway state. Following a short delay of 10 ns, a photon of the third dye laser ( $P_3$ ) further excites molecules from the gateway state to the terminal states below the dissociation threshold. The molecules in the terminal states undergo photofragmentation on the electronic excited surface upon absorbing the second photon, denoted  $P_{3a}$ , from the third laser. We subsequently detect OD radical in the ground state via laser-induced fluorescence (LIF) using a fourth laser pulse. To increase

the detection efficiency, we allow some collisional relaxation of the appearing hot OD fragments by introducing 100 ns delay between the last excitation ( $P_3$ ) and the detection ( $P_4$ ) photons. Monitoring OD fluorescence as a function of the wavenumber of the third laser photon in the sequence, while keeping the wavenumbers of all other lasers fixed, generates a photofragment excitation spectrum. The three-step excitation scheme employed leads to an increase in the overall fraction of molecules promoted to the terminal vibrational level by many orders of magnitude compared to a hypothetical single excitation by a UV laser field of a similar fluence.

The allowed transitions obey rigorous selection rules for the change of the parity  $P$  ( $-1 \leftrightarrow +1$ ), rotational angular momentum  $J$  ( $\Delta J = 0, \pm 1$ ) and its projection  $M$  onto the laboratory  $z$ -axis. The known identity of a gateway state thus provides strict  $J$  and parity values which leaves only two or three options for the  $J$  assignment of the observed final rovibrational states.

In certain cases, we employ  $\Delta M$  selection rules to remove the remaining uncertainty in the  $J$  assignment of transitions from the gateway states with  $J'=1$ . When the third excitation laser is linear polarized parallel to the laboratory  $z$ -axis, which we put in the direction of polarization of the second laser, the selection rules permit transitions to the terminal states with only  $\Delta M = 0$  and  $\Delta J \neq 0$  for  $M = 0$ . For orthogonal polarization of the third laser with respect to the  $z$ -axis, only transitions with  $\Delta M = \pm 1$  are allowed. The implication of these rules is that the  $J=1 \leftarrow J'=1 \leftarrow J''=0$  and  $J = 0 \leftarrow J'=1 \leftarrow J''=0$  two-step transitions are forbidden for parallel and orthogonal laser polarization respectively. Rotation of the polarization plane of the second and/or the third laser by  $90^\circ$  allows us to exclude either

Q(1) or P(1) transitions from a gateway state to the terminal states, making the  $J$ -assignment unambiguous (Figure 2).

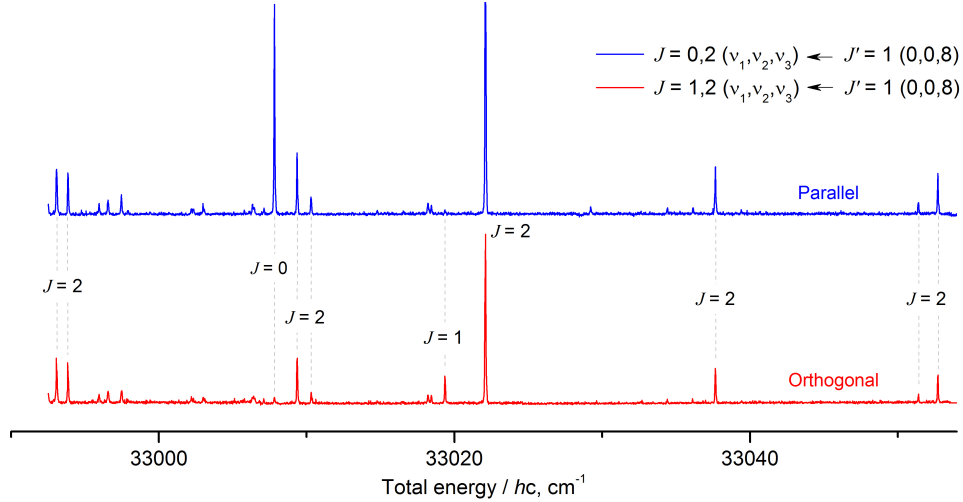


Figure 2: Photofragment spectra of HD<sup>16</sup>O from the gateway state (in normal mode vibrational notation) [25347.43 cm<sup>-1</sup>, 1<sub>0,1</sub>(0,0,8)] to the terminal vibrational state ( $\nu_1, \nu_2, \nu_3$ ) with either  $J=0,2$  (blue) or  $J=1,2$  (red) for parallel and orthogonal polarization of the  $P_3$  laser respectively (see text for details). Corresponding  $J$ -notations of the observed transitions are provided on the plot.

### 3. Experimental data and analysis

The supplementary material to this paper contains files which give the OD and OH bond excitation paths with double or triple resonance and frequencies of the final laser. The energy of intermediate state and the frequency of the final laser gives the values of measured energy levels. These measured levels facilitate the assessment of the accuracy of *ab initio* or semi-empirical PESs. Also it has been shown [36] that the accuracy of the line intensities depend not only on the quality of DMS, but also on the accuracy of ro-vibrational wavefunctions and thus on the accuracy of the PES. The fit of

the PES to the experimental energy levels allows us to improve the quality of the PES and hence the wavefunctions. Such strategy had led to significant success in the study of the main water isotopologue  $\text{H}_2^{16}\text{O}$  [19–25, 42]. In this section we analyze the experimental data, aiming to reproduce the assigned experimental energy levels of HDO. We will use these levels in the subsequent sections for the improvement of the global HDO PES, which we will use for the high temperature line list calculation.

The study of highly excited levels of HDO started from measuring levels of the (1 0 7) vibrational state around  $25\,100\text{ cm}^{-1}$  using techniques similar to those used by us previously [31]. Reproduction of these earlier results with the new experimental setup validated our experimental approach, as well as allowed us to adjust experimental parameters to aid measurements of HDO spectrum at higher energies. Then the higher lying states were studied. The intermediate levels were chosen from (0 0 4) vibrational state around  $14\,000\text{ cm}^{-1}$ . The predictions of  $J=0$  levels were taken from *ab initio* calculations [23] which give predictions in the  $25\,000 - 35\,000\text{ cm}^{-1}$  range with an accuracy of several wavenumbers; the calculated levels lie above the experimental ones with the difference increasing monotonically with energy.

In the  $25\,000 - 35\,000\text{ cm}^{-1}$  region, 210 new energy levels were determined. Their experimental values and assignments are presented in Table 1. Around  $27\,000\text{ cm}^{-1}$  the OH and OD local modes undergo a bifurcation [43, 44] giving birth to so called transversal branches, denoted by a "t" in the Tables 1 and 2. Detailed analysis of this bifurcation is underway. We compared these levels with both *ab initio* calculations, which guided our assignment, and with the calculated levels obtained from our fitted PES (see below). The

small discrepancy for almost all levels between the fitted and the observed ones confirms the assignment presented in the Table 2. Some levels so far have only rotation quantum numbers assigned, vibrational quantum numbers are marked by "X".

Table 1: Experimental energy levels of HDO in comparison with calculated with fitted PES ( $\text{cm}^{-1}$ ).

OH stretch.										
$JK_a K_c$	(0 0 8)	obs.-calc.	(0 0 9)	obs.-calc.	(0 0 10)	obs.-calc.	(X1)	obs.-calc.	(X2)	obs.-calc.
000	25332.716	0.04	27970.198	0.17	30543.017	1.55	33078.186	3.51	33007.820	0.23
101	25347.430	0.01	27984.791	0.16	30557.435	1.57	33093.415	-2.49	33023.249	-0.34
111					30563.929	1.60				
110	25357.881	0.03	27994.765	0.18	30566.998	1.59				
202	25376.102	0.01	28013.127	0.15	30585.430	1.55	33122.051	-0.01	33049.112	0.26
212	25381.113	0.02	28017.726	0.16	30589.680	1.56	33124.663	1.42	33052.067	0.66
221			28054.023	1.47						
303	25417.354	-0.02	28053.844	0.12	30625.590	1.49	33157.447	0.08	33090.641	1.85
313	25420.181	0.02	28056.356	0.15	30627.827	1.48	33160.190	-2.74	33096.353	-1.97
312	25438.697	-0.01								
404	25470.210	-0.03	28105.977	0.10	30677.020	1.44				
414	25471.569	0.01	28107.122	0.11	30677.980	1.40				
505	25534.335	-0.07	28169.266	0.06	30739.366	1.25				
515	25534.937	-0.03	28169.747	0.07	30739.779	1.26				
606	25609.661	-0.03	28243.736	0.00	30812.923	1.31				
616	25609.954	-0.06	28243.892	0.01	30813.040	1.21				
707	25696.814	-0.07	28329.651	-0.05						
717	25696.916	-0.06	28329.651	-0.09						
808	25795.387	0.04	28426.974	0.04						
818	25795.387	-0.09	28426.974	-0.16						
OD stretch.										
$JK_a K_c$	(8 0 0)	obs.-calc.	(9 0 0)	obs.-calc.	(10 0 0)	obs.-calc.	(11 0 0)	obs.-calc.	(13 0 0)	obs.-calc.
000	19414.55	-0.03	21464.49	0.01	23431.73	-0.20	25316.97	-0.39	28823.13	-4.09
101	19427.75	-0.03	21477.40	0.01	23444.38	-0.23	25329.26	-0.46	28834.85	-4.08
111	19441.41	-0.03	21491.07	0.03	23457.95	-0.14	25342.99	-0.40	28848.79	-3.73
110	19443.35	-0.04	21492.90	0.01	23459.70	-0.17	25344.55	-0.44	28850.50	-3.56
202	19453.96	-0.02	21503.03	0.01	23469.35	-0.19	25353.80	-0.43	28858.19	-4.07
212	19465.85	-0.02	21515.02	0.02	23481.46	-0.19	25366.02	-0.42	28870.91	-3.83
211	19471.73	-0.02	21520.56	0.03	23486.70	-0.17	25370.87	-0.36	28874.79	-4.04
221	19512.64	0.01	21561.46	0.06	23527.64	-0.16	25411.80	-0.37	28916.42	-3.97
220	19512.82	0.01	21561.63	0.06	23527.76	-0.19	25411.93	-0.38	28916.52	-3.96
303	19492.78	-0.03	21541.06	0.01	23506.65	-0.20	25390.25	-0.43	28892.90	-3.77
313	19502.37	-0.02	21550.85	0.02	23516.65	-0.19	25400.53	-0.39	28903.61	-4.19
312	19514.11	-0.01	21561.90	0.03	23526.95	-0.24	25410.09	-0.40	28911.85	-4.03
404	19543.70	-0.02	21591.00	0.02	23555.58	-0.23	25438.29	-0.39	28938.80	-3.97
414	19550.87	-0.01	21598.43	0.03	23563.31	-0.22	25446.37	-0.38	28947.88	-3.88
505	19606.19	-0.02	21652.35	0.02	23615.84	-0.21	25497.43	-0.39	28995.58	-4.10
515	19611.16	-0.01	21657.61	0.03	23621.43	-0.20	25503.58	-0.33	29002.52	-4.01
OD stretch.										
$JK_a K_c$	(X3)	obs.-calc.	(14 0 0)	obs.-calc.	(16 0 0)	obs.-calc.	(X4)	obs.-calc.	(17 0 0)	obs.-calc.
000	28979.77	0.66	30455.75	0.36	33452.98	3.74	34273.54	2.73	34815.54	1.25
101	28992.19	0.97	30467.15	0.37	33463.87	0.76	34284.98	-2.57	34825.93	1.76
111	29009.60	-0.50	30481.16	0.29	33478.18	1.99	34300.84	-2.93	34840.53	-8.97
110	29012.09	-0.46	30482.32	0.31	33478.92	-0.83	34302.83	1.87	34840.98	-9.56
202	29016.85	0.22	30489.90	0.40	33485.61	-1.94	34307.66	-2.74	34847.38	-3.48
212	29032.20	-0.50	30502.81	0.31	33499.21	-2.24	34321.10	0.30	34861.71	0.20
211	29039.35	-0.13	30506.31	0.38	33501.46	-2.33	34327.02	-0.65	34863.02	-2.68

*Continued on next page...*

$JK_a K_c$	(X3)	obs.-calc.	(14 0 0)	obs.-calc.	(16 0 0)	obs.-calc.	(X4)	obs.-calc.	(17 0 0)	obs.-calc.
221	29091.63	0.35	30548.27	0.35	33544.30	-2.42	34375.61	2.68	34906.39	5.79
220	29091.87	0.46	30548.34	0.35	33544.34	-0.94	34375.80	2.75	34906.40	1.02
303	29052.88	0.25	30523.83	0.44	33518.14	-1.12	34341.44	1.84	34879.44	-0.49
313	29065.77	-0.24	30535.23	0.33	33530.74	-1.22	34351.75	2.17	34892.89	2.15
312	29074.81	-1.23	30542.19	0.44	33535.23	0.33	34363.50	3.46	34895.57	-1.99
404	29100.80	0.60	30568.74	0.49	33561.36	0.09	34386.28	0.33	34922.07	-1.98
414	29108.01	1.68	30578.36	0.35	33572.73	-0.92	34392.97	2.31	34934.67	2.38
505			30624.37	0.52	33615.13	-0.67	34432.72	-1.45	34975.25	1.88
515			30632.14	0.36	33625.12	0.73	34444.63	-1.93	34987.01	-4.15

#### 4. Potential energy surface fit

In order to perform a fit of the HDO PES, the rotation-vibration Schrödinger equation has to be solved. For that purpose we used the DVR3D program suite [45]. DVR3D uses an exact representation of nuclear motion kinetic energy operator so that, within constraints of the Born-Oppenheimer approximation, any uncertainty in the wavefunctions is due to the PES and any failure of the Born-Oppenheimer approximation. Because of the lower symmetry of HDO and the higher density of states, achieving accuracy in HDO calculations comparable to that routinely achieved for H<sub>2</sub><sup>16</sup>O requires the diagonalisation of significantly larger matrices.

Nuclear motion calculations were performed in Radau coordinates with the  $z$ -axis embedded close to the OH bond direction. The discrete variable representation (DVR) basis comprised 50 Gauss-Laguerre points in each radial coordinate and 48 (associated) Gauss-Legendre points in the angular coordinate. Basis set parameters for the radial coordinates were taken from Yurchenko *et al.* [32]. The final Hamiltonian matrix was of dimension 7000. For each rotational state  $J$ , two Hamiltonian matrices were diagonalized with dimensions  $1100 \times (J + 1)$  and  $1100 \times J$ , depending on their overall parity. Only the levels with  $J=0, 2$  and  $5$  were included to the fits.

Initially we attempted to fit all the data from 0 to 35 000 cm<sup>-1</sup> using a single functional form. Yurchenko *et al.* [46] proposed using not only empirical molecular energy levels, but also the results of an *ab initio* calculations in the optimization procedure. Inclusion of *ab initio* energies in the optimization procedure allows one to restrict the discrepancy between the semi-empirical PES and the *ab initio* potential, which suppresses spurious behavior of the

PES in regions not well-characterized by the experimental data, and to make the procedure more flexible since a larger number of parameters can be varied. To use this method we fitted previously-calculated *ab initio* points [22] alongside the 804 HDO experimental energy levels with  $J=0, 2$  and  $5$  from [28] up to  $25\,000\text{ cm}^{-1}$  and the 108 energy levels with  $J=0, 2$  and  $5$  determined in this work in the  $25\,000\text{ cm}^{-1}$  to  $35\,000\text{ cm}^{-1}$  region.

As the overall accuracy of the fit was not satisfactory (several wavenumbers up to  $35\,000\text{ cm}^{-1}$ ), we decided to use the fitted PES we obtained as the starting upper potential  $V_{\text{up}}$  in the energy-switching procedure described in the following subsection. As data below  $25\,000\text{ cm}^{-1}$  will be represented by the lower part of potential  $V_{\text{low}}$  (see below), to fit  $V_{\text{up}}$  we used the following weighting procedure. Levels in the  $25\,000 - 35\,000\text{ cm}^{-1}$  region obtained in this work were given unit weight whereas levels below  $25\,000\text{ cm}^{-1}$  were weighted  $0.1$ . The resulting PES ( $V_{\text{up}}$ ) gave a standard deviation for levels above  $25\,000\text{ cm}^{-1}$  of about  $1\text{ cm}^{-1}$  and about  $0.1\text{ cm}^{-1}$  for the much more numerous lower levels. To put this result into perspective we note that we achieved an accuracy of  $0.1\text{ cm}^{-1}$ , but only up to  $15\,000\text{ cm}^{-1}$ , for all water isotopologues five years ago using purely *ab initio* methods [47]. Thus this PES is global but less accurate for lower levels than necessary.

#### *4.1. Energy-switching for $\text{HD}^{16}\text{O}$ potential energy surface*

The determination of new experimental levels in the  $25\,000 - 35\,000\text{ cm}^{-1}$  region gave us the opportunity to significantly improve the accuracy of the *ab initio* PES by fitting it to the newly obtained experimental data. To preserve the high accuracy of  $0.035\text{ cm}^{-1}$  with the existing semi-empirical PES for the levels below  $25\,000\text{ cm}^{-1}$  [32] and to extend the range of the PES to  $35\,000$

$\text{cm}^{-1}$  we use the method of Varandas [48, 49] and make a composite PES from two different potentials of HDO on the basis of an energy-switching procedure.

As the base potential we took the fitted HDO07 PES due to Yurchenko *et al.* [32] as the most accurate available semi-empirical HDO PES. This PES is valid up to  $25\,000\text{ cm}^{-1}$ . To give a more accurate description of higher lying levels this potential was extended by combining with a less accurate, global PES. To do this we adopted a switching function of the form advocated by Varandas [48].

$$V_{\text{global}} = V_{\text{low}}f(E) + V_{\text{up}}(1 - f(E)). \quad (1)$$

The function  $f(E)$  changes monotonically from 1 to 0 around the fixed value  $E_0$  over a region of about  $1000\text{ cm}^{-1}$ . The initial  $V_{\text{up}}$  was the fitted global PES described above.

Table 2: Measured HDO vibrational band origins compared to calculated with new PES in  $\text{cm}^{-1}$ .

State	Obs.	Calc.	Obs.-Calc.
(0 1 0)	1403.48	1403.50	-0.016
(1 0 0)	2723.68	2723.71	-0.032
(0 2 0)	2782.01	2782.02	-0.009
(0 0 1)	3707.47	3707.47	-0.003
(1 1 0)	4099.96	4099.98	-0.024
(0 3 0)	4145.47	4145.48	-0.007

*Continued on next page...*

State	Obs.	Calc.	Obs.-Calc.
(0 1 1)	5089.54	5089.55	-0.008
(2 0 0)	5363.82	5363.84	-0.016
(0 4 0)	5420.04	5420.00	0.042
(1 0 1)	6415.46	6415.48	-0.018
(0 2 1)	6451.90	6451.91	-0.011
(0 5 0)	6690.41	6690.42	-0.007
(2 1 0)	6746.91	6746.92	-0.013
(0 0 2)	7250.52	7250.51	0.009
(0 3 1)	7754.61	7754.39	0.215
(1 1 1)	7808.76	7808.76	-0.001
(0 6 0)	7914.32	7914.32	-0.003
(3 0 0)	7918.17	7918.18	-0.008
(0 1 2)	8611.10	8611.08	0.022
(2 0 1)	9047.07	9047.08	-0.012
(1 2 1)	9155.82	9155.82	-0.002
(3 1 0)	9293.00	9293.05	-0.048
(1 5 0)	9381.79	9381.78	0.006
(2 3 0)	9487.92	9487.91	0.005
(0 2 2)	9934.79	9934.75	0.039
(1 0 2)	9967.02	9967.00	0.023
(4 0 0)	10378.95	10378.97	-0.019
(0 0 3)	10631.68	10631.70	-0.017
(0 3 2)	11242.92	11242.90	0.023

*Continued on next page...*

State	Obs.	Calc.	Obs.-Calc.
(1 1 2)	11315.43	11315.39	0.044
(2 2 1)	11701.78	11701.80	-0.024
(4 1 0)	11754.58	11754.62	-0.038
(1 7 0)	11773.31	11773.28	0.032
(3 3 0)	11958.56	11958.60	-0.043
(0 1 3)	11969.75	11969.76	-0.007
(5 0 0)	12767.14	12767.21	-0.068
(0 2 3)	13278.36	13278.36	-0.002
(1 0 3)	13331.61	13331.62	-0.014
(0 0 4)	13853.63	13853.70	-0.072
(5 1 0)	14147.43	14147.48	-0.049
(1 1 3)	14660.72	14660.73	-0.008
(6 0 0)	15065.71	15065.81	-0.098
(0 1 4)	15166.10	15166.11	-0.006
(1 4 2)	15170.95	15171.00	-0.049
(0 2 4)	16456.19	16456.21	-0.018
(1 0 4)	16539.04	16539.09	-0.051
(0 0 5)	16920.02	16920.03	-0.006
(0 1 5)	18208.45	18208.37	0.076
(8 0 0)	19414.55	19414.57	-0.022
(0 0 6)	19836.88	19836.76	0.123
(9 0 0)	21464.49	21464.48	0.012
(1 0 6)	22454.48	22454.48	-0.002

*Continued on next page...*

State	Obs.	Calc.	Obs.-Calc.
(0 0 7)	22625.53	22625.38	0.148
(10 0 0)	23431.73	23431.94	-0.207
(1 0 7)	25140.85	25140.79	0.057
(11 0 0)	25316.97	25317.35	-0.384
(0 0 8)	25332.72	25332.68	0.036
(12 0 0)	27124.89	27124.12	0.773
(0 0 9)	27970.20	27970.03	0.168
(13 0 0)	28823.13	28827.22	-4.087
(14 0 0)	30455.75	30455.39	0.362
(0 0 10)t	30543.02	30541.46	1.559
(16 0 0)	33452.98	33449.239	3.741
(17 0 0)	34815.54	34814.29	1.249

The final fit of  $V_{\text{up}}$  was performed as follows. To reduce the influence of the upper part of the PES on levels below 25 000  $\text{cm}^{-1}$  the switching energy was chosen much higher than the upper limit of validity of HDO07 PES:  $E_0=35\,000\text{ cm}^{-1}$ . This means that  $V_{\text{up}}$  starts to influence lower lying levels only around 20 000  $\text{cm}^{-1}$ . Fixing  $V_{\text{low}}$  with the form of Eq. (1) distorted levels between 20 000  $\text{cm}^{-1}$  and 35 000  $\text{cm}^{-1}$ . In order to get a satisfactory final result we refitted  $V_{\text{up}}$  using the energy-switching form of Eq. (1) with unit weights for all experimental levels between 25 000 and 35 000  $\text{cm}^{-1}$  and levels below 25 000  $\text{cm}^{-1}$  weighted 0.1.

Results of the final fit for  $J=0$  levels are given in Table 2. The final standard deviation  $\sigma$  of the fitted levels up to 25 000  $\text{cm}^{-1}$  is 0.043  $\text{cm}^{-1}$  and

above 25 000  $\text{cm}^{-1}$  it is 1.91  $\text{cm}^{-1}$ . The accuracy of the levels present in the calculated line list (see next section) but not included in the fit is illustrated in Table 3. Table 3 that the accuracy of the fit is uniform in  $J$  and not affected by our decision, on the grounds of computational cost, to perform the fit using data for only three  $J$  values. The files to compile the DVR3D program with new semi-empirical PES are provided in the supplementary materials.

Table 3: Standard deviation,  $\sigma$  in  $\text{cm}^{-1}$ , of the HDO IUPAC [28] energy levels with respect to energies obtained from variational nuclear motion computations using the PES of this work.  $N$  gives the number of levels used in each comparison.

$J$	$N$	$\sigma$
0	54	0.0419
1	176	0.0465
2	302	0.0479
3	421	0.0427
4	523	0.0525
5	599	0.0439
6	657	0.0443
7	677	0.0463
8	676	0.0441
9	640	0.0466
10	574	0.0464
11	467	0.0386
12	408	0.0396
13	360	0.0395
14	296	0.0417
15	263	0.0427
16	232	0.0476
17	204	0.0503
18	164	0.0524
19	137	0.0527
20	74	0.0575

## 5. Line list calculation

To calculate the linestrengths, the initial,  $|i\rangle$  and final,  $|f\rangle$  rotation-vibration wavefunctions as well as the components of the dipole moment surfaces (DMS),  $\mu_\alpha$  are required. For water, the DMS comprises a two-dimensional vector, since there is no component of the dipole perpendicular to the plane of the molecule. The wavefunctions and corresponding line strengths of the HDO linelist were generated with the program suite DVR3D [45].

To reduce the computer time required for the calculation of the line list we choose a slightly smaller basis set than that used in the fitting procedure – 40 radial DVR points, 48 angular DVR points and the dimension of the final matrix 7000. The decrease in the number of radial grid points changes the energy levels below 25 000  $\text{cm}^{-1}$  by less than by 0.001  $\text{cm}^{-1}$ . The levels around 35 000  $\text{cm}^{-1}$  change by about 0.01  $\text{cm}^{-1}$  which is much less than residuals in this region. The calculations were performed for  $J$  up to 20 and the considered energy levels up to 35 000  $\text{cm}^{-1}$ . For the room temperature line list a minimum intensity at 100% abundance was chosen around  $1 \times 10^{-30}$   $\text{cm}^{-1}/(\text{cm}^{-2}\text{molecule})$  at 296 K. As the same calculations will be used in the future as the basis of a global high temperature line list with  $J$  up to 50, much lower intensity lines were also retained.

Initially we computed HDO line list using the best then available DMS: LTP2011 due to Lodi, Tennyson and Polyansky [34]. However, while the calculations were in progress, a new, more accurate water DMS, named CKAPTEN, became available [38]. The CKAPTEN DMS was constructed using the finite-field method within the Born-Oppenheimer approximation with a

relativistic correction to BO energies, such that it is mass independent. This means that the DMS should be equally valid for all isotopologues of water. We therefore redid the intensity calculations using the CKAPTEN DMS assuming that this DMS will give more accurate intensities for HDO as it has found for main water isotopologue [40]. However, there is a lack of high accuracy data on HDO transitions intensities for us to directly validate this assumption.

Table 4: Comparison of  $1_{01} - 0_{00}$  transition intensities, in  $\text{cm}^{-1}/(\text{cm}^{-2}\text{molecule})$  at 296 K, (with powers of 10 in parenthesis) for first bands of HDO calculated with different DMSs: CKAPTEN [38] and LTP2011 [34]. The difference,  $\Delta$ , is the percentage change between CKAPTEN and LTP2001.

Band	Frequency $\text{cm}^{-1}$	$I(\text{CKAPTEN})$	$I(\text{LTP2011})$	$\Delta$ %
(010)	1419.05	2.58(-20)	2.58(-20)	0.13
(100)	2738.95	1.36(-20)	1.37(-20)	-0.97
(020)	2797.61	1.63(-21)	1.64(-21)	-0.72
(001)	3722.89	2.28(-20)	2.31(-20)	-1.30
(200)	5378.78	1.08(-21)	1.07(-21)	0.23
(002)	7265.83	1.43(-21)	1.41(-21)	0.90

Table 4 compares intensities for some low-lying IR transitions calculated with the different DMSs. One can see that for low-lying transitions, intensities change by about 1 percent. As found for  $\text{H}_2^{16}\text{O}$  [38], UV transition intensities change very significantly when the DMS used is changed from LTP2011 to CKAPTEN. Atmospheric studies in the near UV [41] confirm that the higher intensities given by the CKAPTEN DMS are necessary to obtain agreement with the atmospheric observations. Thus we expect that use of CKAPTEN DMS will not only improve the intensities of the lines in IR and optical region, but will significantly improve the intensities of the calculated lines of HDO in the UV region as well. High resolution intensities

measurements would be very helpful in confirming this assumption.

Our line list was prepared in ExoMol format [50]: a states file with 230 000 energy levels, quantum numbers and/or other information (where available), and a transitions file with 2 800 000 lines which contains  $A_{ij}$ -coefficients. The size of states and transitions files is about 100 MB. Ftp site <http://www.tampa.phys.ucl.ac.uk/ftp/astrodata/water/BT2/> contain a FORTRAN program, SPECTRA-BT2.F90, that will enable users to generate emission or absorption spectra from ExoMol format by specifying various parameters including temperature, frequency range, cut-off intensity and linewidth. To further improve the line list we substitute variationally calculated levels by the experimentally-determined energy levels of HDO given by the IUPAC study [28] and in this work. The file with mixed calculated and experimental energy levels can be used as an alternative or improvement on the pure variational energies in the construction of a line list for a given temperature using the energy levels file provided in the supplementary materials which can be done using the program ExoCross [51]. The supplementary materials contain one transitions file and two states files, one with pure variational energies and the other with experimental levels inserted instead of variational ones where possible.

## 6. Conclusion

We present new experimental results that probe much higher energy levels of HD<sup>16</sup>O than those available from previous studies. These data are used to construct a potential energy surface which is valid over a much more extended energy range than those available previously for this system. This new surface is then used as the basis for computing HDO line lists using

two available *ab initio* dipole moment surfaces. These line lists have the virtue of being complete for the intensity cutoffs specified at 296 K. We also believe that in nearly all the cases they represent the best available data for this isotopologue; the exception being the cases, where there are direct, high accuracy measurements of individual lines. We therefore recommend our line list, which is based on the CKAPTEN DMS, to be used as the basis for generating the HD<sup>16</sup>O spectra in future releases of atmospheric databases. This work, when combined with the previous study by Lodi and Tennyson [52] on H<sub>2</sub><sup>17</sup>O and H<sub>2</sub><sup>18</sup>O means that hybrid, HITRAN-style line lists are now available for all the most important isotopologues of water.

Of course, the process of constructing a line list for a given molecule is one of continuing improvement. Work on improving and extending the list of empirical energy levels for water using the MARVEL (measured active vibration rotation energy levels) procedure for H<sub>2</sub><sup>16</sup>O [53] and the H<sub>2</sub><sup>17,18</sup>O isotopologues [54] has just been completed. A comprehensive update of the available [28] HD<sup>16</sup>O MARVEL energy levels is currently in progress. When this is completed the current line list will be processed and included as part of the ExoMol project [55, 56].

The recent MARVEL studies on H<sub>2</sub>O employ variational calculations to generate so-called pseudo-experimental energy levels [17]; use of this procedure significantly expands the numbers of levels known with almost experimental accuracy. These levels can be included in the line list for the minor isotopogues [54, 57]. Work on generating pseudo-experimental levels of HD<sup>17</sup>O and HD<sup>18</sup>O using the PES developed here is currently underway. Furthermore, recent comparisons with the results of the high quality exper-

iments for H<sub>2</sub>O [35, 40] suggest the areas, where the *ab initio* intensity predictions should be further improved. Work in this direction is also underway. Improvements in the model, and in particular the potential energy surface, used to compute the vibration-rotation wavefunctions will reduce problems with computed transition intensities which can be characterized as unstable due to the inadequate treatment of resonance interactions [52, 58]; this will allow a greater proportion of the transition intensities to be predicted reliably *ab initio*.

Finally, the global study of the HDO spectrum is important from the viewpoint of the bifurcation analysis [43, 44]. For that purpose the analysis of experimental data on HDO up to dissociation is required. Work on this is in progress.

## Acknowledgments

The reported study was funded by The Russian Fund for Basic Research under research project Nos 18-02-00577 (NFZ, DSM and OLP); State project 0030-2021-0016 (VYM and MAK); ERC Advanced Investigator Project 883830 and the UK Natural Environment Research Council grant NE/T000767/1; and by the Swiss National Science Foundation (grant 200020\_172522).

## References

- [1] S. Jousaume, R. Sadourny, J. Jouzel, A general circulation model of water isotope cycles in the atmosphere, *Nature* 311 (5981) (1984) 24–29.
- [2] M. Ridal, A. Jonsson, M. Werner, D. P. Murtagh, A one-dimensional simulation of the water vapor isotope hdo in the tropical stratosphere,

- Journal of Geophysical Research: Atmospheres 106 (D23) (2001) 32283–32294.
- [3] G. A. Schmidt, G. Hoffmann, D. T. Shindell, Y. Hu, Modeling atmospheric stable water isotopes and the potential for constraining cloud processes and stratosphere-troposphere water exchange, *Journal of Geophysical Research: Atmospheres* 110 (D21).
- [4] C. Frankenberg, K. Yoshimura, T. Warneke, I. Aben, A. Butz, N. Deutscher, D. Griffith, F. Hase, J. Notholt, M. Schneider, et al., Dynamic processes governing lower-tropospheric HDO/H<sub>2</sub>O ratios as observed from space and ground, *Science* 325 (2009) 1374–1377.
- [5] K. Yoshimura, C. Frankenberg, J. Lee, M. Kanamitsu, J. Worden, T. Röckmann, Comparison of an isotopic atmospheric general circulation model with new quasi-global satellite measurements of water vapor isotopologues, *Journal of Geophysical Research: Atmospheres* 116 (D19).
- [6] X. Zhang, X. Zhang, H. Guan, Y. Huang, H. Wu, Spatiotemporal distributions of  $\delta D$  in atmospheric water vapor based on TES Data during 2004–2009, *Acta Meteorologica Sinica* 26 (2012) 683–699.
- [7] H. Boesch, N. M. Deutscher, T. Warneke, K. Byckling, A. J. Cogan, D. W. T. Griffith, J. Notholt, R. J. Parker, Z. Wang, HDO/H<sub>2</sub>O ratio retrievals from GOSAT, *Atmos. Meas. Tech. Discuss* (2012) 6643–6677.
- [8] K. Yoshimura, Stable water isotopes in climatology, meteorology, and hydrology: A review, *Journal of the Meteorological Society of Japan. Ser. II* 93 (2015) 513–533.

- [9] M. Werner, B. Haese, X. Xu, X. Zhang, M. Butzin, G. Lohmann, Glacial–interglacial changes in  $\text{H}_2^{18}\text{O}$ , HDO and deuterium excess—results from the fully coupled ECHAM5/MPI-OM Earth system model, *Geoscientific Model Development* 9 (2016) 647–670.
- [10] T. Fouchet, E. Lellouch, Vapor pressure isotope fractionation effects in planetary atmospheres: Application to deuterium, *Icarus* 144 (2000) 114–123.
- [11] F. Montmessin, T. Fouchet, F. Forget, Modeling the annual cycle of HDO in the Martian atmosphere, *Journal of Geophysical Research: Planets* 110.
- [12] C. De Bergh, B. Bezard, T. Owen, D. Crisp, J.-P. Maillard, B. L. Lutz, Deuterium on Venus: observations from Earth, *Science* 251 (1991) 547–549.
- [13] D. Bockelée-Morvan, D. Gautier, D. Lis, K. Young, J. Keene, T. Phillips, T. Owen, J. Crovisier, P. F. Goldsmith, E. A. Bergin, et al., Deuterated water in comet C/1996 B2 (Hyakutake) and its implications for the origin of comets, *Icarus* 133 (1998) 147–162.
- [14] G. L. Villanueva, M. J. Mumma, B. P. Bonev, R. E. Novak, R. J. Barber, M. A. Di Santi, Water in planetary and cometary atmospheres:  $\text{H}_2\text{O}/\text{HDO}$  transmittance and fluorescence models, *Journal of Quantitative Spectroscopy and Radiative Transfer* 113 (2012) 202–220.
- [15] R. J. Barber, J. Tennyson, G. J. Harris, R. N. Tolchenov, A high ac-

- curacy computed water line list, *Mon. Not. R. Astron. Soc.* 368 (2006) 1087–1094.
- [16] O. L. Polyansky, A. A. Kyuberis, N. F. Zobov, J. Tennyson, S. N. Yurchenko, L. Lodi, ExoMol molecular line lists XXX: a complete high-accuracy line list for water, *Mon. Not. R. Astron. Soc.* 480 (2018) 2597–2608. doi:10.1093/mnras/sty1877.
- [17] O. L. Polyansky, A. A. Kyuberis, L. Lodi, J. Tennyson, R. I. Ovsyanikov, N. Zobov, ExoMol molecular line lists XIX: high accuracy computed line lists for  $\text{H}_2^{17}\text{O}$  and  $\text{H}_2^{18}\text{O}$ , *Mon. Not. R. Astron. Soc.* 466 (2017) 1363–1371. doi:10.1093/mnras/stw3125.
- [18] B. A. Voronin, J. Tennyson, R. N. Tolchenov, A. A. Lugovskoy, S. N. Yurchenko, A high accuracy computed line list for the HDO molecule, *Mon. Not. R. Astron. Soc.* 402 (2010) 492–496.
- [19] P. Maksyutenko, J. S. Muentzer, N. F. Zobov, S. V. Shirin, O. L. Polyansky, T. R. Rizzo, O. V. Boyarkin, Approaching the full set of energy levels of water, *The Journal of Chemical Physics* 126 (2007) 241101. doi:10.1063/1.2748751.
- [20] M. Grechko, P. Maksyutenko, N. F. Zobov, S. V. Shirin, O. L. Polyansky, T. R. Rizzo, O. V. Boyarkin, Collisionally assisted spectroscopy of water from 27 000 to 34 000  $\text{cm}^{-1}$ , *J. Phys. Chem. A* 112 (2008) 10539–10545. doi:10.1021/jp805849q.
- [21] M. Grechko, O. V. Boyarkin, T. R. Rizzo, P. Maksyutenko, N. F. Zobov, S. Shirin, L. Lodi, J. Tennyson, A. G. Császár, O. L. Polyansky, State-

- selective spectroscopy of water up to its first dissociation limit, *J. Chem. Phys.* 131 (2009) 221105.
- [22] A. G. Császár, E. Mátyus, T. Szidarovszky, L. Lodi, N. F. Zobov, S. V. Shirin, O. L. Polyansky, J. Tennyson, Ab initio prediction and partial characterization of the vibrational states of water up to dissociation, *J. Quant. Spectr. Rad. Transfer* 111 (2010) 1043–1064.
- [23] N. F. Zobov, S. V. Shirin, L. Lodi, B. C. Silva, J. Tennyson, A. G. Császár, O. L. Polyansky, First-principles rotation-vibration spectrum of water above dissociation, *Chem. Phys. Lett.* 507 (2011) 48–51.
- [24] O. L. Polyansky, N. F. Zobov, I. I. Mizus, L. Lodi, S. N. Yurchenko, J. Tennyson, A. G. Császár, O. V. Boyarkin, Global spectroscopy of the water monomer, *Phil. Trans. Royal Soc. London A* 370 (2012) 2728–2748.
- [25] O. V. Boyarkin, M. A. Koshelev, O. Aseev, P. Maksyutenko, T. R. Rizzo, N. F. Zobov, L. Lodi, J. Tennyson, O. L. Polyansky, Accurate bond dissociation energy of water determined by triple-resonance vibrational spectroscopy and ab initio calculations, *Chem. Phys. Lett.* 568-569 (2013) 14–20.
- [26] A. Jenouvrier, M. F. Marienne, M. Carleer, R. Colin, A.-C. Vandaele, P. F. Bernath, O. L. Polyansky, J. Tennyson, The visible and near ultraviolet overtone spectrum of HOD, *J. Mol. Spectrosc.* 209 (2001) 165–168.
- [27] B. A. Voronin, O. V. Naumenko, M. Carleer, P.-F. Coheur, S. Fally, A. Jenouvrier, R. N. Tolchenov, A. C. Vandaele, J. Tennyson, HDO

- absorption spectrum above  $11500\text{ cm}^{-1}$ : Assignment and dynamics, *J. Mol. Spectrosc.* 244 (2007) 87–101.
- [28] J. Tennyson, P. F. Bernath, L. R. Brown, A. Campargue, M. R. Carleer, A. G. Császár, L. Daumont, R. R. Gamache, J. T. Hodges, O. V. Naumenko, O. L. Polyansky, L. S. Rothman, R. A. Toth, A. C. Vandaele, N. F. Zobov, A. Z. Fazliev, T. Furtenbacher, I. E. Gordon, S. N. Mikhailenko, B. A. Voronin, IUPAC critical Evaluation of the Rotational-Vibrational Spectra of Water Vapor. Part II. Energy Levels and Transition Wavenumbers for  $\text{HD}^{16}\text{O}$ ,  $\text{HD}^{17}\text{O}$ , and  $\text{HD}^{18}\text{O}$ , *J. Quant. Spectr. Rad. Transfer* 111 (2010) 2160–2184. doi:10.1016/j.jqsrt.2010.06.012.
- [29] A. Janca, K. Tereszchuk, P. F. Bernath, N. F. Zobov, S. V. Shirin, O. L. Polyansky, J. Tennyson, Emission spectrum of hot HDO below  $4000\text{ cm}^{-1}$ , *J. Mol. Spectrosc.* 219 (2003) 132–135.
- [30] T. Parekunnel, P. F. Bernath, N. F. Zobov, S. V. Shirin, O. L. Polyansky, J. Tennyson, Emission spectrum of hot HDO in the  $380 - 2190\text{ cm}^{-1}$  region, *J. Mol. Spectrosc.* 210 (2001) 28–40.
- [31] P. Theule, A. Callegari, T. R. Rizzo, J. Muentner, Dipole moments of HDO in highly excited vibrational states measured by Stark induced photofragment quantum beat spectroscopy, *J. Chem. Phys.* 122 (2005) 124312. doi:10.1063/1.1864912.
- [32] S. N. Yurchenko, B. A. Voronin, R. N. Tolchenov, N. Doss, O. V. Nau-

- menko, W. Thiel, J. Tennyson, Potential energy surface of HDO up to 25000  $\text{cm}^{-1}$ , J. Chem. Phys. 128 (2008) 044312.
- [33] L. Lodi, J. Tennyson, Theoretical methods for small-molecule rovibrational spectroscopy, J. Phys. B: At. Mol. Opt. Phys. 43 (2010) 133001.
- [34] L. Lodi, J. Tennyson, O. L. Polyansky, A global, high accuracy *ab initio* dipole moment surface for the electronic ground state of the water molecule, J. Chem. Phys. 135 (2011) 034113. doi:10.1063/1.3604934.
- [35] M. Birk, G. Wagner, J. Loos, L. Lodi, O. L. Polyansky, A. A. Kyuberis, N. F. Zobov, J. Tennyson, Accurate line intensities for water transitions in the infrared: comparison of theory and experiment, J. Quant. Spectr. Rad. Transfer 203 (2017) 88–102. doi:10.1016/j.jqsrt.2017.03.040.
- [36] I. I. Mizus, A. A. Kyuberis, N. F. Zobov, V. Y. Makhnev, O. L. Polyansky, J. Tennyson, High accuracy water potential energy surface for the calculation of infrared spectra, Phil. Trans. Royal Soc. London A 376 (2018) 20170149. doi:10.1098/rsta.2017.0149.
- [37] A. A. Kyuberis, N. F. Zobov, O. V. Naumenko, B. A. Voronin, O. L. Polyansky, L. Lodi, A. Liu, S.-M. Hu, J. Tennyson, Room temperature line lists for deuterated water, J. Quant. Spectr. Rad. Transfer 203 (2017) 175–185. doi:10.1016/j.jqsrt.2017.06.026.
- [38] E. K. Conway, A. A. Kyuberis, O. L. Polyansky, J. Tennyson, N. Zobov, A highly accurate *ab initio* dipole moment surface for the ground elec-

- tronic state of water vapour for spectra extending into the ultraviolet, *J. Chem. Phys.* 149 (2018) 084307. doi:10.1063/1.5043545.
- [39] E. K. Conway, I. E. Gordon, A. A. Kyuberis, O. L. Polyansky, J. Tennyson, N. F. Zobov, Accurate line lists for  $\text{H}_2^{16}\text{O}$ ,  $\text{H}_2^{18}\text{O}$  and  $\text{H}_2^{17}\text{O}$  with extensive comparisons to theoretical and experimental sources including the HITRAN2016 database, *J. Quant. Spectr. Rad. Transfer* 241 (2020) 106711. doi:10.1016/j.jqsrt.2019.106711.
- [40] E. K. Conway, I. E. Gordon, J. Tennyson, O. L. Polyansky, S. N. Yurchenko, K. Chance, A semi-empirical potential energy surface and line list for  $\text{H}_2^{16}\text{O}$  extending into the near-ultraviolet, *Atmos. Chem. Phys.* 20 (2020) 10015–10027. doi:10.5194/acp-20-10015-2020.
- [41] J. Lampel, D. Pöhler, O. L. Polyansky, A. A. Kyuberis, N. F. Zobov, J. Tennyson, L. Lodi, U. Frieß, Y. Wang, S. Beirle, U. Platt, T. Wagner, Detection of water vapour absorption around 363 nm in measured atmospheric absorption spectra and its effect on DOAS evaluations, *Atmos. Chem. Phys.* 17 (2017) 1271–1295. doi:10.5194/acp-2016-388.
- [42] M. Grechko, O. V. Boyarkin, T. R. Rizzo, P. Maksyutenko, N. F. Zobov, S. V. Shirin, L. Lodi, J. Tennyson, A. G. Csaszar, O. L. Polyansky, State-selective spectroscopy of water up to its first dissociation limit, *J. Chem. Phys.* 131 (2009) 221105. doi:10.1063/1.3273207.
- [43] F. Mauguiere, V. Tyuterev, S. C. Farantos, Bifurcation effects and patterns in the vibrational excited states of isotopi-

- cally substituted water, *Chem. Phys. Lett.* 494 (2010) 163–169. doi:10.1016/j.cplett.2010.06.0279.
- [44] F. Mauguiere, M. Rey, V. Tyuterev, J. Suarez, S. C. Farantos, A Periodic Orbit Bifurcation Analysis of Vibrationally Excited Isotopologues of Sulfur Dioxide and Water Molecules: Symmetry Breaking Substitutions, *J. Phys. Chem. A* 114 (2010) 9836–9847. doi:10.1021/jp1030569.
- [45] J. Tennyson, M. A. Kostin, P. Barletta, G. J. Harris, O. L. Polyansky, J. Ramanlal, N. F. Zobov, DVR3D: a program suite for the calculation of rotation-vibration spectra of triatomic molecules, *Comp. Phys. Comm.* 163 (2004) 85–116.
- [46] S. N. Yurchenko, M. Carvajal, P. Jensen, F. Herregodts, T. R. Huet, Potential parameters of PH<sub>3</sub> obtained by simultaneous fitting of ab initio data and experimental vibrational band origins, *J. Chem. Phys.* 290 (2003) 59–67.
- [47] O. L. Polyansky, R. I. Ovsyannikov, A. A. Kyuberis, L. Lodi, J. Tennyson, N. F. Zobov, Calculation of rotation-vibration energy levels of the water molecule with near-experimental accuracy based on an ab initio potential energy surface, *J. Phys. Chem. A* 117 (2013) 9633–9643. doi:10.1021/jp312343z.
- [48] B. R. L. Galvão, S. P. J. Rodrigues, A. J. C. Varandas, Energy-switching potential energy surface for the water molecule revisited: A highly accurate singled-sheeted form, *J. Chem. Phys.* 129 (2008) 044302.

- [49] C. M. R. Rocha, A. J. . Varandas, Energy-switching potential energy surface for ground-state, *Chem. Phys. Lett.* 700 (2018) 36 – 43. doi:10.1016/j.cplett.2018.04.005.
- [50] J. Tennyson, C. Hill, S. N. Yurchenko, Data structures for ExoMol: Molecular line lists for exoplanet and other atmospheres, in: 6<sup>th</sup> international conference on atomic and molecular data and their applications ICAMDATA-2012, Vol. 1545 of AIP Conference Proceedings, AIP, New York, 2013, pp. 186–195. doi:10.1063/1.4815853.
- [51] S. N. Yurchenko, A. F. Al-Refaie, J. Tennyson, ExoCross: A general program for generating spectra from molecular line lists, *Astro. Astrophys.* 614 (2018) A131. doi:10.1051/0004-6361/201732531.
- [52] L. Lodi, J. Tennyson, Line lists for H<sub>2</sub><sup>18</sup>O and H<sub>2</sub><sup>17</sup>O based on empirically-adjusted line positions and ab initio intensities, *J. Quant. Spectr. Rad. Transfer* 113 (2012) 850–858. doi:10.1016/j.jqsrt.2012.02.023.
- [53] T. Furtenbacher, R. Tóbiás, J. Tennyson, O. L. Polyansky, A. G. Császár, W2020: A Database of Validated Rovibrational Experimental Transitions and Empirical Energy Levels of H<sub>2</sub><sup>16</sup>O, *J. Phys. Chem. Ref. Data* 49 (2020) 033101.
- [54] T. Furtenbacher, R. Tóbiás, J. Tennyson, O. L. Polyansky, A. A. Kyuberis, R. I. Ovsyannikov, N. F. Zobov, A. G. Császár, W2020: A Database of Validated Rovibrational Experimental Transitions and Empirical Energy Levels Part II. H<sub>2</sub><sup>17</sup>O and H<sub>2</sub><sup>18</sup>O with an

- Update to H<sub>2</sub><sup>16</sup>O, J. Phys. Chem. Ref. Data 49 (2020) 043103.  
doi:10.1063/5.0030680.
- [55] J. Tennyson, S. N. Yurchenko, ExoMol: molecular line lists for exoplanet and other atmospheres, Mon. Not. R. Astron. Soc. 425 (2012) 21–33.  
doi:10.1111/j.1365-2966.2012.21440.x.
- [56] J. Tennyson, S. N. Yurchenko, A. F. Al-Refai, V. H. J. Clark, K. L. Chubb, E. K. Conway, A. Dewan, M. N. Gorman, C. Hill, A. E. Lynas-Gray, T. Mellor, L. K. McKemmish, A. Owens, O. L. Polyansky, M. Semenov, W. Somogyi, G. Tinetti, A. Upadhyay, I. Waldmann, Y. Wang, S. Wright, O. P. Yurchenko, The 2020 release of the ExoMol database: molecular line lists for exoplanet and other hot atmospheres, J. Quant. Spectr. Rad. Transfer 255 (2020) 107228.  
doi:10.1016/j.jqsrt.2020.107228.
- [57] L. K. McKemmish, T. Masseron, J. Hoeijmakers, V. V. Pérez-Mesa, S. L. Grimm, S. N. Yurchenko, J. Tennyson, ExoMol Molecular line lists – XXXIII. The spectrum of Titanium Oxide, Mon. Not. R. Astron. Soc. 488 (2019) 2836–2854.
- [58] E. J. Zak, J. Tennyson, O. L. Polyansky, L. Lodi, S. A. Tashkun, V. I. Perevalov, A room temperature CO<sub>2</sub> line list with *ab initio* computed intensities, J. Quant. Spectr. Rad. Transfer 177 (2016) 31–42.  
doi:10.1016/j.jqsrt.2015.12.022.